Evaluation of electro-optic, elasto-optic, piezoelectric, and elastic coefficients of Ba0.77Ca0.23TiO3 through orientation dependent photorefractive beam coupling

Sylvie Bernhardt, Lauren Mize, Philippe Delaye, Gérald Roosen

Evaluation of electro-optic, elasto-optic, piezoelectric, and elastic coefficients of $Ba_{0.77}Ca_{0.23}TiO_3$ through orientation dependent photorefractive beam coupling

Sylvie Bernhardt, Lauren Mize, Philippe Delaye,[a] and Gérald Roosen
Laboratoire Charles Fabry de l'Institut d'Optique, Unité Mixte de Recherche 8501 du Centre National de la Recherche Scientifique/Université Paris-Sud, Bat. 503, Centre Scientifique d'Orsay, 91403 Orsay Cedex, France

(Received 22 April 2002; accepted 29 August 2002)

We present a demonstration of the influence of the indirect electro-optic effect on the photorefractive performance of $Ba_{0.77}Ca_{0.23}TiO_3$ (BCT). The comparison of the orientation dependence of the two-beam coupling energy transfer gain with theoretical model allows us to obtain information on the electro-optic coefficients, but also an evaluation of the unknown elasto-optic, piezoelectric, and elastic stiffness coefficients of BCT. We found $r_{13}^T = 33\ \mathrm{pm\,V^{-1}}$ and $r_{33}^T = 170\ \mathrm{pm\,V^{-1}}$. These values are in good agreement with other published values. For the interesting coefficient r_{42}^T, we find a higher value $r_{42}^T = 465\ \mathrm{pm\,V^{-1}}$ than the one previously published. From this study we also determine that as in the case of $BaTiO_3$, the optimal orientation is given by a 45°-cut BCT. © *2002 American Institute of Physics.* [DOI: 10.1063/1.1515950]

I. INTRODUCTION

$Ba_{0.77}Ca_{0.23}TiO_3$ (BCT) is a very promising photorefractive material, which is expected to replace barium titanate in many industrial applications. Indeed, contrary to barium titanate, it has no phase transition around room temperature. Nevertheless, the interest of this crystal for applications will depend on its photorefractive gain. Moreover, to implement a device such as a double phase conjugate mirror (DPCM), it is interesting to have an idea of the configuration for which the gain is maximum.

In a first approximation, the photorefractive gain can be calculated from the electro-optic coefficients. But, it has been shown in Ref. 1 that the contribution of the indirect electro-optic effects (piezoelectric, elasto-optic, elastic stiffness) in crystals such as barium titanate is important. BCT is close to barium titanate and this contribution has certainly to be taken into account to evaluate the gain. Nevertheless, the growth of BCT is relatively recent and most of the parameters necessary for calculating the indirect electro-optic contributions are unknown.

Therefore, we present here an optical characterization of this crystal. We first present the classical model used to evaluate the electro-optic coefficients of photorefractive crystals and its limitations. This leads to the realization of further experiments presented in the second part, that show that the indirect electro-optic effect has to be taken into account. In a third part, we theoretically study the influence of the indirect electro-optic effect and then determine the effective electro-optic coefficients by comparison of the experimental results to this model, from which we evaluate the values of the electro-optic, elasto-optic, piezoelectric, and elastic coefficients of BCT. We finally determine the best configuration that maximizes the gain in BCT.

II. CLASSICAL TWO-BEAM COUPLING EXPERIMENTS

The simplest experiment to characterize photorefractive crystals is the two-beam coupling experiment. The energy transfer that appears in this experiment is measured as a function of experimental parameters such as the grating spacing, the incident illumination, the input polarization orientation, or the crystal orientation. This gives information on the charge transport mechanism as well as on crystal parameters such as the electro-optic coefficients. Nevertheless, this kind of measurement, despite being very informative, is not self-consistent considering the great number of material parameters that are necessary to theoretically calculate the photorefractive gain. In well known crystals such as barium titanate or gallium arsenide most of the needed parameters are known from the literature, and the comparison between theory and experiment is easier. In the case of a recently discovered material like BCT most of the needed parameters are unknown, and the comparison between theory and experiment is difficult. Nevertheless, as we will show in the following, it is possible, with some simple approximations, to extract some information from photorefractive measurements not only on optical parameters (such as the electro-optic coefficients), but also on nonoptical parameters (such as the piezoelectric coefficients).

A. Experimental setup

The two-beam coupling experimental setup is presented in Fig. 1. The beam from a laser is divided in two by a glass plate. The transmitted beam is a powerful beam called the pump beam. The reflected beam is a weak beam called the signal beam. Both beams are sent on the photorefractive crystal where they interfere and create an index grating on which they diffract. The $\pi/2$ phase shift between the index

[a]Author to whom all correspondence should be addressed; electronic mail: philippe.delaye@iota.u-psud.fr

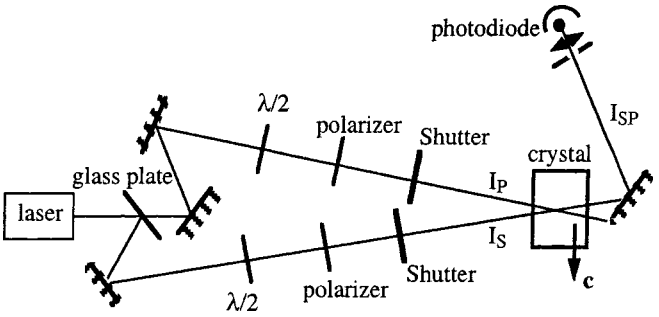

FIG. 1. Two-beam coupling setup.

grating and the illumination pattern, characteristic of the photorefractive effect, leads to an energy transfer between the two beams (Fig. 2).

From the steady state intensities of the transmitted weak signal beam without and with illumination by the pump beam, we calculate the photorefractive gain Γ thanks to the relation

$$\Gamma = \frac{1}{\ell} \ln \frac{I_{SP}}{I_S}, \tag{1}$$

where ℓ is the length of the crystal, I_{SP} is the signal intensity after the energy transfer, and I_S the signal intensity before the energy transfer.

In this kind of experiment, the *c* axis of the crystal is in the plane of incidence defined by the beams and the orientation is characterized by the two angles θ and β (defined inside the crystal), where 2θ is the angle between the beams inside the crystal and β is the angle between the grating wave vector and the *c* axis (Fig. 3).

Classical photorefractive experiments are performed with $\beta=0$ and, therefore, the grating wave vector is aligned parallel to the *c* axis of the crystal. We will use this configuration in our first experiments.

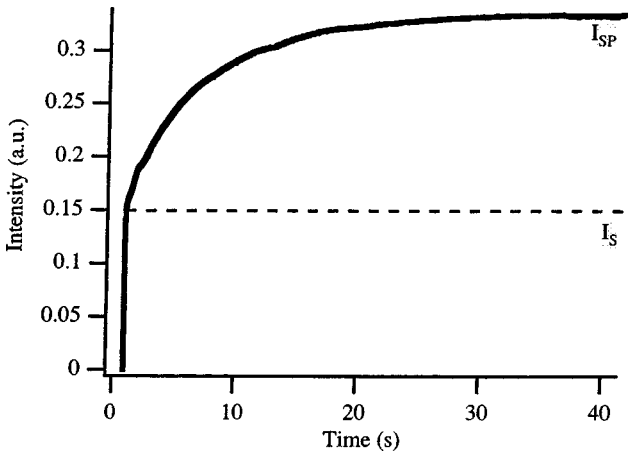

FIG. 2. Energy transfer from the pump beam toward the signal beam.

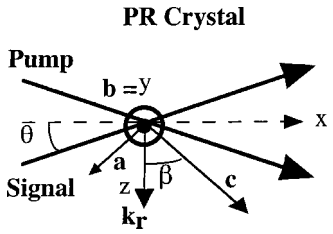

FIG. 3. Orientation of the crystal.

B. Theoretical expression of photorefractive gain

By measuring the dependence of the gain with the grating wave vector, we will be able to determine the electro-optic coefficients of the crystal as given by the theoretical expression of the photorefractive gain

$$\Gamma = \frac{2\pi}{\lambda_0} n^3 r^{\text{eff}} E_{SC}(k_r, I)(\hat{e}_S \cdot \hat{e}_P), \tag{2}$$

where λ_0 is the wavelength in vacuum, *n* the mean refractive index, and r^{eff} the effective electro-optic coefficient. The term $(\hat{e}_S \cdot \hat{e}_p)$ is the scalar product between the unit vectors which are aligned parallel to the electric field of the two beams. It depends only on the polarization of the beams and is equal to 1 or $\cos(2\theta)$ whether the beams are ordinary or extraordinary polarized. The dependence of the photorefractive gain with the grating wave vector $k_r = 4\pi n \sin\theta/\lambda_0$ and with incident intensity I comes from the space-charge field and is generally described by the following formula[2,3]:

$$E_{SC}(k_r, I) = \frac{k_B T}{e} \eta(I) \frac{k_r}{1 + \frac{k_r^2}{k_0^2(I)}}. \tag{3}$$

$\eta(I)$ expresses the saturation of the gain with intensity, which is related to the ratio between photoconductivity and dark conductivity and is written as

$$\eta(I) = \frac{1}{1 + \frac{I_{\text{sat}}}{I}}. \tag{4}$$

In Eq. (3), the second term depending on intensity is the Debye screening wave vector k_0, which depends on the effective trap density as

$$k_0^2(I) = \frac{e^2 N_{\text{eff}}(I)}{k_B T \epsilon_0 \epsilon^{\text{eff}}}, \tag{5}$$

where ϵ^{eff} is the effective dielectric constant.

In the configuration chosen for our experiments ($\beta=0$), the effective electro-optic coefficient for each polarization expresses as

$$r_0^{\text{eff}} = r_{13}, \tag{6}$$

$$r_e^{\text{eff}} = \tfrac{1}{2}[r_{13}(\cos(2\theta) - 1) + r_{33}(\cos(2\theta) + 1)]. \tag{7}$$

And the effective dielectric constant is written as $\epsilon^{\text{eff}} = \epsilon_{33}$, when $\beta=0$.

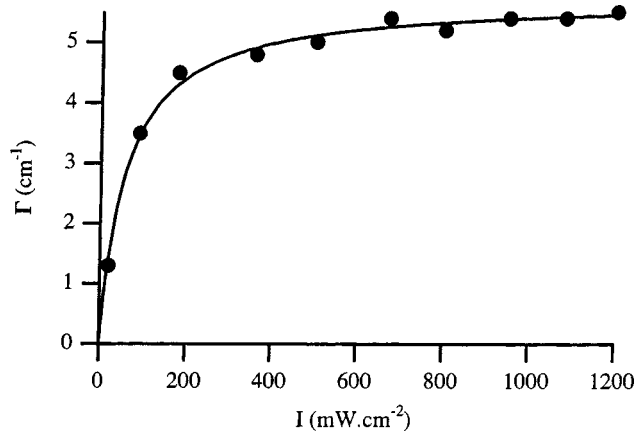

FIG. 4. Dependence of the gain with intensity for a grating spacing of 0.6 μm and for $\beta=0$ with ordinary polarization. The line represents an adjustment with a function of the form of Eq. (4).

C. Experimental results

We perform two-beam coupling experiments as a function of the grating wave vector in a 0°-cut BCT crystal labeled B69 in a configuration where $\beta=0$.[4] The crystal has been grown at the University of Osnabrück and prepared by F. E. E. GmbH. The dimensions of the sample are $a\times b\times c = 1.76\,\text{mm}\times 4.74\,\text{mm}\times 3.48\,\text{mm}$, where c is the optical axis direction. In all the experiments, we use a frequency-doubled Nd:YAG laser at 532 nm. From the energy transfer we measure Γ from Eq. (1). In order to be sure that we saturate the photorefractive gain, we have measured the gain versus incident illumination. The criterion for saturation is that gain should not depend on illumination and we have selected a large enough value of the incident intensity to be saturated. From the measured values reported in Fig. 4, the gain is constant as soon as the intensity is higher than 500 mW cm^{-2}. It reaches half of its maximum for an intensity I_{sat} of 50 mW cm^{-2}. All the following experiments have been performed with an intensity of 1.2 W cm^{-2} and thus with $\eta(I)=1$. Each measurement datum in Fig. 5 corresponds to a measurement in attenuation and in amplification allowing to separate the photorefractive components from an eventual absorption component (induced absorption or absorption grating).

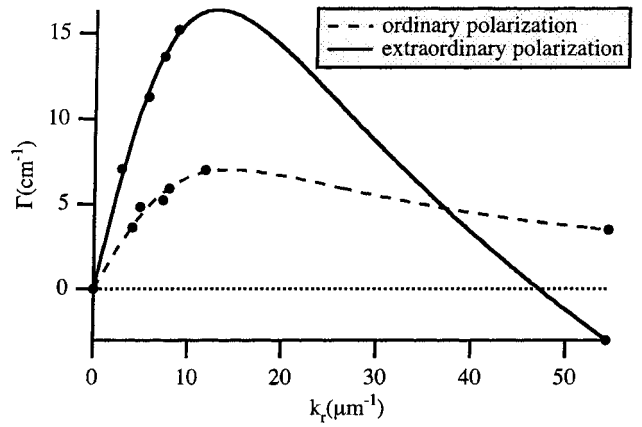

FIG. 5. Experimental photorefractive gain Γ as a function of the grating spacing for ordinary and extraordinary polarizations.

The grating spacing dependence curves (Fig. 5) are adjusted with expressions (2) and (3). According to Eq. (6), we obtained $r_{13}=(22\pm 0.3)\,\text{pm V}^{-1}$ and $k_0=1.44\times 10^7\,\text{m}^{-1}$ from the experiment with ordinary polarization. Then, using these results and Eq. (7), we obtained $r_{33}=(55\pm 0.6)\,\text{pm V}^{-1}$ from the experiment with extraordinary polarization. The effective trap density can be determined from k_0^2 according to Eq. (5) using the value of ϵ_{33} from Ref. 5, we have $N_{\text{eff}}=7.0\times 10^{22}\,\text{m}^{-3}$.

D. Approximations and their validity

In these experiments, we needed to make several approximations due to the fact that BCT is a recently grown crystal and that we knew almost nothing about its properties. Therefore, we supposed that:

(1) the crystal is perfectly poled;
(2) there is no electron-hole competition;
(3) the intensity saturation follows the simple law given by Eq. (4); and
(4) the indirect electro-optic effects are negligible.

If the crystal is not perfectly poled, some 180° ferroelectric domains could persist in the crystal that would lead to the apparition of an additional reduction factor in the gain expression.[6] Identically, if electron-hole competition exists in the crystal, it would appear as a reduction coefficient ξ_0[7] in the space-charge field expression [Eq. (3)]. The gain might also be reduced by a factor $\eta(I)$ due to a complex dependence of the gain with intensity because of secondary traps.[8] The observed saturation of the gain with intensity might then be only an intermediary plateau, that precedes the real saturation, leading to a value of $\eta(I)$ smaller than 1 at the used intensities.

The indirect electro-optic effect comes from the fact that the electric field changes the refractive index through the electro-optic effect but also through a combination of the piezoelectric and elasto-optic effect. As we will explain in the next part, the indirect electro-optic effect leads to a complex dependence of the effective electro-optic coefficients on β, with a value of the effective electro-optic coefficient at $\beta=0$ which is no more exactly equal to r_{13}.

We thus see that neglecting these effects might lead to an underestimation of the theoretical value of the photorefractive gain. Nevertheless, there is a difference between the different corrections. The first three always lead to a reduction of the gain that is independent of the orientation of the crystal, and that may vary from sample to sample. The last correction is not necessarily a decrease of the effect. Moreover, it depends on the orientation of the crystal and it will be the same whatever the sample.

The measurement presented above and performed with a single orientation in a single rather unknown crystal does not enable us to check the validity of our approximations. We will thus need further experiments on another sample and with different orientations.

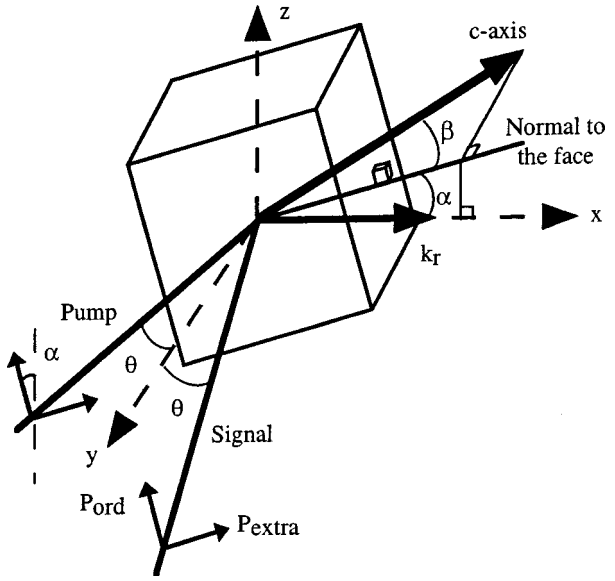

FIG. 6. Orientation of the incident beams and the *c* axis. The angles are defined inside the crystal.

III. ORIENTATION DEPENDENCE OF PHOTOREFRACTIVE GAIN

A simple experiment can bring a lot of information on the photorefractive characteristics of a crystal. It was first proposed and used by Zgonik, Nakagawa, and Günter.[1]

Two symmetrical beams forming an angle 2θ inside the material symmetrically enter the crystal, which then turns around the normal to the crystal (y axis) (Fig. 6). The angle of rotation is α. We start with $\alpha=0°$ and then the c axis is in the (x,y) plane. β is defined as the angle between the c axis and its projection on the $(z-x)$ plan. θ and β are defined inside the crystal. As previously, from the energy transfer we measure the photorefractive gain as a function of the rotation angle α. To always enter the crystal with eigen polarizations (ordinary or extraordinary), the polarizations are rotated by the same angle α. We use an argon laser at 514.5 nm with an intensity sufficient to saturate the photorefractive gain.

The space-charge field amplitude depends on the rotation angle α because of ϵ_{eff} in k_0 [Eq. (5)]. To minimize this dependence, we performed experiments with a small grating wave vector (2.5 μm^{-1}) to have $k_0^2 \gg k_r^2$. Then, the gain is approximately proportional to the grating wave vector

$$\Gamma \approx \frac{2\pi}{\lambda_0} n^3 r^{\text{eff}} \frac{k_B T}{e} k_r \tag{8}$$

and the measurement of the dependence of the gain with α with a fixed angle θ gave us directly the dependence of the effective electro-optic coefficient r^{eff} with α. This precaution is taken to facilitate the interpretation of the experimental curves, but is not a necessity. In the theoretical comparison presented in the following the complete expression of the gain is used.

According to the usual model of the photorefractive effect[9] (without the indirect electro-optic effect), the dependence of the effective electro-optic coefficient and thus of the gain Γ with α should have a sinusoidal form. Indeed, we would have for a 0°-cut crystal ($\beta=0$), for ordinary and extraordinary polarization

$$r_0^{\text{eff}}(\alpha) = r_{13} \cos \alpha, \tag{9}$$

$$r_e^{\text{eff}}(\alpha) = (r_{13}(\sin\theta)^2 + r_{33}(\cos\theta)^2)\cos\alpha. \tag{10}$$

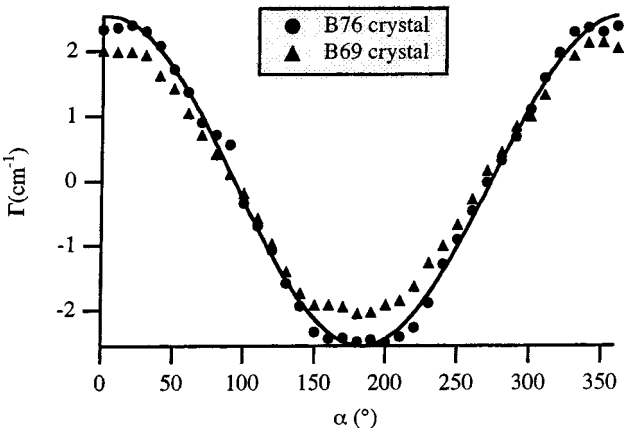

FIG. 7. Gain as a function of the rotation angle α for the crystals labeled B69 and B76 with ordinary polarized beams. The line presents the theoretical curve without taking into account the indirect electro-optic effect.

Two crystals were used in the experiment, the B69 sample previously characterized and a second BCT sample, labeled B-76.10.1.2. This second sample is a 1000 ppm rhodium doped sample with dimensions $a \times b \times c = 1.61\,\text{mm} \times 4\,\text{mm} \times 4.75\,\text{mm}$. Both crystals were 0° cut. The experimental curves obtained might be slightly dissymmetric between negative and positive gains because of an absorption component (induced absorption or absorption gratings). These absorption components are small compared to the photorefractive gain (<10%) so we have corrected this dissymmetry to present in the following only the photorefractive gain.

On the experimental curves for ordinary polarization (Fig. 7) and for extraordinary polarization (Fig. 8), we see that the data depart from the theoretical sinusoidal shape. This indicates that the indirect electro-optic effect has to be

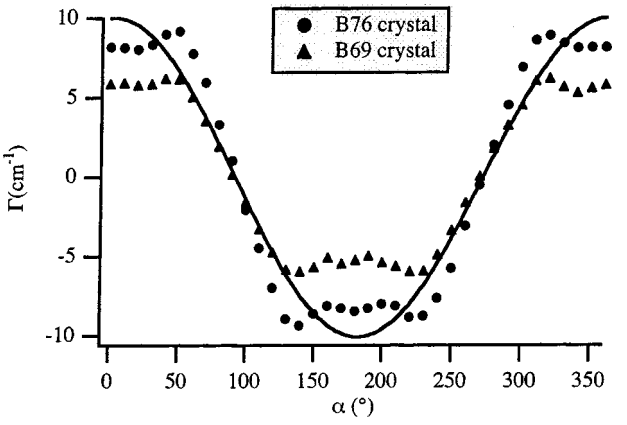

FIG. 8. Gain as a function of the rotation angle α for the crystals labeled B69 and B76 with extraordinary polarized beams. The line presents the theoretical curve without taking into account the indirect electro-optic effect.

taken into account in BCT as it has been considered in $BaTiO_3$.[1] Before going further and comparing the experimental curves to the theoretical model, several preliminary remarks can be made on these curves. First, compared to the experimental curves obtained in $BaTiO_3$,[1] the curves measured in BCT are closer to a sinusoidal shape indicating that the influence of the indirect electro-optic effect seems to be less important in BCT than in $BaTiO_3$. Then, the shape of the curves for both samples is the same except for a different amplitude (with a ratio between samples similar for both polarization). This indicates that a sample dependent, orientation independent reduction coefficient is present on at least one (if not on two) of the samples.

IV. DETERMINATION OF INDIRECT ELECTRO-OPTIC EFFECT COEFFICIENTS

We will now compare the experimental rotation data to the theoretical model, that will allow us to determine some optical parameters (electro- and elasto-optic coefficients) but also mechanical parameters (piezoelectric, elastic stiffness coefficients) of BCT.

A. Indirect electro-optic effect

The indirect electro-optic effect is well known in the study of electro-optic modulators. It leads to the definition of two electro-optic coefficients, the clamped r_{ij}^S and the unclamped r_{ij}^T electro-optic coefficients, which intervene as the measurement is performed at low or high frequencies.[10] The question is thus soon asked whether it was the clamped or the unclamped electro-optic coefficient that has to be used in the expression describing the photorefractive effect. In fact, a closer look at the physics of the electro-optic materials under spatially modulated electric field showed that in the case of the photorefractive effect, one has to use an effective electro-optic coefficient, depending of the symmetry and the orientation of the crystal,[11,12] which in general is neither equal to the clamped electro-optic coefficient, nor to the unclamped one.

The electric field changes the refractive index through the electro-optic effect but also through the piezoelectric and elasto-optic effects. Both contributions appear in the variation of the optic ellipsoid[11,12]

$$\Delta\left(\frac{1}{n^2}\right)_{ij}=r_{ijk}^S E_k+p_{ijkl}'^E u_{kl}, \tag{11}$$

where r_{ijk}^S is the clamped electro-optic coefficient, u_{kl} is the displacement gradient matrix of the deformation of the crystal induced by the piezoelectric effect. The term $p_{ijkl}'^E$ equals $p_{ijkl}^E+p_{ij[kl]}^E$ with p_{ijkl}^E the elasto-optic coefficients at constant field and $p_{ij[kl]}^E$ the roto-optic effect. However, in $BaTiO_3$, the roto-optic contribution is rather small.[13] Therefore $[p'^E]$ can be assimilated to $[p^E]$ for $BaTiO_3$ (the same approximation will be made for BCT). After calculating the deformation u_{kl} taking into account that it is produced by a periodically spatially modulated space-charge electric field $\mathbf{E}=E_{sc}\mathbf{n}\cos(\mathbf{k}_r\cdot\mathbf{r})$ (oriented along the direction $\mathbf{n}$ of the grating vector $\mathbf{k}_r=k_r\mathbf{n}$), we arrive to

$$\Delta\left(\frac{1}{n^2}\right)_{ij}=r_{ij}^{\mathrm{eff}}E_{sc}\cos(\mathbf{k}_r\cdot\mathbf{r})$$
$$=(r_{ijk}^S n_k+p_{ijkl}^E n_1 A_{km}^{-1}B_m)E_{sc}\cos(\mathbf{k}_r\cdot\mathbf{r}) \tag{12}$$

with

$$A_{ik}=c_{ijkl}^E n_j n_l \quad \text{and} \quad B_i=e_{kij}n_k n_j, \tag{13}$$

where c_{ijkl}^E is the elastic stiffness at constant field and e_{ijk} the piezoelectric coefficient; $\mathbf{n}$ is written in a coordinate system linked to the crystallographic axis (a,b,c) as

$$\mathbf{n}=\begin{pmatrix} n_1 \\ n_2 \\ n_3 \end{pmatrix}=\begin{pmatrix} \cos\alpha\sin\beta \\ \sin\alpha \\ \cos\alpha\cos\beta \end{pmatrix}. \tag{14}$$

The analytical expressions for the effective electro-optic coefficients (for ordinary and extraordinary polarizations, respectively) are

$$r_0^{\mathrm{eff}}=r_{22}^{\mathrm{eff}}(\alpha,\beta), \tag{15}$$

$$r_e^{\mathrm{eff}}=\tfrac{1}{2}\{r_{11}^{\mathrm{eff}}(\alpha,\beta)[\cos(2\theta)-\cos(2\beta)]+2r_{13}^{\mathrm{eff}}(\alpha,\beta)$$
$$\times\sin(2\beta)+r_{33}^{\mathrm{eff}}(\alpha,\beta)[\cos(2\theta)+\cos(2\beta)]\}. \tag{16}$$

These expressions are similar to the usual ones obtained without the indirect electro-optic effect[9] if we simply replace $r_{13}\cos\beta$ by $r_{22}^{\mathrm{eff}}(\alpha,\beta)$ in r_0^{eff} and $r_{13}\cos\beta$ by $r_{11}^{\mathrm{eff}}(\alpha,\beta)$, $r_{42}\sin\beta$ by $r_{13}^{\mathrm{eff}}(\alpha,\beta)$ and $r_{33}\cos\beta$ by $r_{33}^{\mathrm{eff}}(\alpha,\beta)$ in r_e^{eff}. The parameters determined in part II [Eqs. (6) and (7)] for a 0°-cut crystal, are still valid but their expression with the crystal parameters is different. Indeed, instead of determining r_{13} and r_{33}, we have determined $r_{22}^{\mathrm{eff}}(0,0)=r_{11}^{\mathrm{eff}}(0,0)=r_{13}^S+p_{13}^E e_{33}/c_{33}^E$ and $r_{33}^{\mathrm{eff}}(0,0)=r_{33}^S+p_{33}^E e_{33}/c_{33}^E$.

We also define an effective dielectric constant $\epsilon^{\mathrm{eff}}(\alpha,\beta)$ that is calculated from the clamped dielectric constant ϵ_{ij}^S taking into account the piezoelectric and elasto-optic contributions

$$\epsilon^{\mathrm{eff}}(\alpha,\beta)=\epsilon_{ij}^S n_i n_j+\epsilon_0^{-1}e_{ijk}e_{mnl}n_i n_j n_m n_n A_{kl}^{-1}. \tag{17}$$

According to these equations, many parameters (at least 21) intervene in the calculation of the indirect electro-optic effect and most of them are unknown in BCT. We thus have developed a model to calculate them from our general knowledge about perovskite ferroelectrics of the family of $BaTiO_3$ and BCT.

B. Theoretical determination of direct and indirect electro-optic effects

Above about 100 °C, $BaTiO_3$ and BCT are in a cubic phase ($m3m$ symmetry) and when the temperature decreases, they go into a tetragonal phase (4 mm) (until 5 °C for $BaTiO_3$ and down to at least −120 °C for BCT). During this phase change, a spontaneous polarization P_S appears, that will bias the third order effects (such as Kerr effect and electrostriction) to transform them into second order effects (Pockels effect and piezoelectric effect, respectively).[14] We will use this property to calculate all the unknown parameters we need to evaluate the indirect electro-optic influence on the photorefractive effect.[4] The main advantage of this

procedure is that it reduces the number of parameters of the calculation from 21 to 16, some of which being known from the literature. In the following all the calculations are performed using the contracted notation except when precised.

The first step of the calculation gives the value of the spontaneous polarization from[15]

$$\Delta n = -\tfrac{1}{2} n^3 (g_{11}^S - g_{12}^S) P_S^2 + \Delta n_0(T) \tag{18}$$

with the Kerr coefficients g_{ij}^S, the refractive index n and the birefringence Δn, which were measured in BCT.[16] $\Delta n_0(T)$ is a temperature dependent structural contribution from the high temperature phase, that is negligible in the case in $BaTiO_3$, and will be considered such in BCT.[15] Concerning the Kerr coefficients, it has been shown that they are the same for all the perovskites,[15] so we take, as initial values, the one determined for $BaTiO_3$.[17]

Once the spontaneous polarization is determined, we calculate the piezoelectric tensors d_{ij} and b_{ij} from

$$\begin{cases} d_{31} = \epsilon_0(\epsilon_{33}^T - 1) b_{31} = 2\epsilon_0(\epsilon_{33}^T - 1) Q_{12} P_s \\ d_{33} = \epsilon_0(\epsilon_{33}^T - 1) b_{33} = 2\epsilon_0(\epsilon_{33}^T - 1) Q_{11} P_s \\ d_{24} = \epsilon_0(\epsilon_{11}^T - 1) b_{24} = \epsilon_0(\epsilon_{11}^T - 1) Q_{44} P_s \end{cases} \tag{19}$$

using the known value of the unclamped dielectric constant ϵ_{ii}^T of BCT.[5] For the electrostriction coefficient Q_{ij}, we use as initial values the values determined in $BaTiO_3$,[15,18] considering the close relationship of BCT with $BaTiO_3$.

Then we determine the elastic compliance at constant electric field s_{ij}^E using the relation

$$s_{ij}^E = s_{ij}^P + b_{ki} d_{kj} \tag{20}$$

with s_{ij}^P the elastic compliance at constant polarization (with the values of $BaTiO_3$[19] taken as initial values as in the case of the electrostriction coefficient). The elastic stiffness c_{ij}^E is deduced from the relation between the strain τ and the stress σ

$$\tau_i = c_{ij}^E \sigma_j \quad \text{and} \quad \sigma_i = s_{ij}^E \tau_j \tag{21}$$

which allows the calculation of the piezoelectric tensor e_{ij}

$$e_{ij} = d_{ik} c_{kj}^E . \tag{22}$$

We then deduce the clamped ϵ_{ii}^S dielectric constants[13]

$$\epsilon_0 \epsilon_{ii}^S = \epsilon_0 \epsilon_{ii}^T - e_{ij} d_{ij} . \tag{23}$$

Now, we can calculate the clamped electro-optic coefficients using[15]

$$\begin{cases} r_{13}^S = 2\epsilon_0(\epsilon_{33}^S - 1) g_{12}^S P_s \\ r_{33}^S = 2\epsilon_0(\epsilon_{33}^S - 1) g_{11}^S P_s \\ r_{42}^S = \epsilon_0(\epsilon_{11}^S - 1) g_{44}^S P_s \end{cases} \tag{24}$$

and the unclamped electro-optic coefficients

$$r_{ij}^T = r_{ij}^S + p_{ik}^E d_{jk} . \tag{25}$$

The elasto-optic coefficient at constant electric field p_{ij}^E is given, in the tensorial notation, by[17]

$$p_{ijmn}^E = p_{ijmn}^p + 2(g_{ij3k}^S P_s) \cdot e_{kmn} \tag{26}$$

using, here also, the value of the elasto-optic coefficient at constant polarization p_{ij}^p of $BaTiO_3$.

TABLE I. Final set of parameters determined for BCT. The parameters that have changed compared to the initial set of parameters (see Ref. 4) are indicated in bold characters.

	Initial value	Final values
$g_{11}^S (\times 10^{-2}\ \mathrm{m^4\ C^{-2}})$	15±3	**11**
$g_{12}^S (\times 10^{-2}\ \mathrm{m^4\ C^{-2}})$	3.8±0.6	**3.5**
$g_{44}^S (\times 10^{-2}\ \mathrm{m^4\ C^{-2}})$	7±1.5	**13.5**
p_{11}^P	0.37±0.03	0.37±0.03
p_{12}^P	0.11±0.01	0.11±0.01
p_{66}^P	−0.30±0.15	−0.30±0.15
$s_{11}^P (\times 10^{-12}\ \mathrm{m^2\ N^{-1}})$	8.7	8.7
$s_{12}^P (\times 10^{-12}\ \mathrm{m^2\ N^{-1}})$	−3.35	−3.35
$s_{66}^P (\times 10^{-12}\ \mathrm{m^2\ N^{-1}})$	8.9	8.9
$Q_{11} (\mathrm{m^4\ C^{-2}})$	0.09	0.09
$Q_{12} (\mathrm{m^4\ C^{-2}})$	−0.04	−0.04
$Q_{44} (\mathrm{m^4\ C^{-2}})$	0.06	0.06
Δn	0.05	0.05
n	2.46	2.46
ϵ_{11}^T	1120±30	1120±30
ϵ_{33}^T	240±10	240±10

The numerical values of the cubic phase parameters we use are presented in Table I. With this initial set of parameters, and the relations (18)–(26) coupled with relations (12)–(17) giving the effective electro-optic coefficient, we are now able to calculate the theoretical variation of the photorefractive gain with the rotation angle α, that we will compare to the experimental results presented in Sec. III.

C. Comparison with experimental results

The first operation is a simple comparison of the experimental data with the theoretical curves. The result is shown in Fig. 9 for sample B69 for ordinary polarization. We see that the shape of the curve is correct but that the amplitude is greater for the theoretical curve, with the same result observed for the extraordinary polarization. We thus deduce that the introduction of an orientation independent correction factor is necessary to explain the experimental results, even if at this level of the study we are unable to determine the exact nature of this reduction factor (depoling of the crystal, electron-hole competition, lack of intensity saturation of the

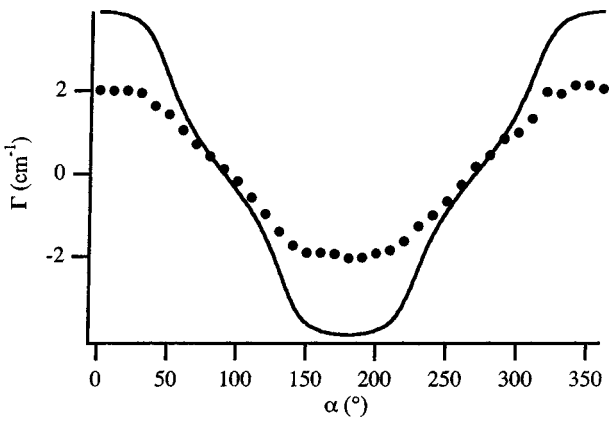

FIG. 9. Comparison between simulation (full line) and experimental results (dots) for the B69 crystal with ordinary polarization.

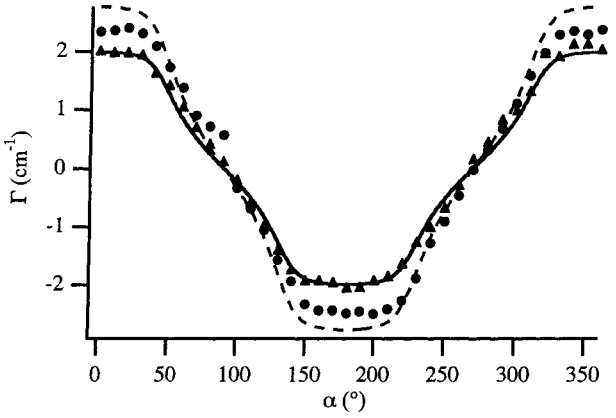

FIG. 10. Comparison between simulations with optimized parameters (full and dashed lines) and experimental results for the B69 (triangles) and B76 (dots) crystals with ordinary polarization.

gain). The correct shape of the curves is an indication that the initial set of parameters we use is not far from the actual one.

Going further, we first compensate the theoretical curves for the reduction factor equal to 0.7 for the B76.10.1.2 crystal and 0.5 for the B69 crystal, and we made an adjustment of the theoretical curves to the experimental data. Due to the fact that the initial set of parameters already allows a good description of the experimental curves and because of the great number of parameters, we do not make an extensive study and we make the adjustment by changing the smallest number of parameters. These fits are performed simultaneously on both polarizations and crystals. It means that we have adjusted four curves simultaneously. The best accordance (Figs. 10 and 11) between the experimental points and the simulations is obtained by only slightly changing g_{11}^S and g_{12}^S to $g_{11}^S = 0.11\,\mathrm{m}^4\,\mathrm{C}^{-2}$ and $g_{12}^S = 0.035\,\mathrm{m}^4\,\mathrm{C}^{-2}$ (Table I, column 2). We note that the resulting values are still in the error bars announced in Ref. 17.

Besides parameters such as g_{44}^S (through r_{42}) that are not intervening in the expression of the effective electro-optic coefficient in the 0°-cut crystal configuration we use, some parameters have little influence. We note that only p_{11}^P, s_{11}^P, and Q_{12} have a real influence on the shape of the curves (Fig. 12). This low influence of some of the parameters and also the fact that some parameters can eventually compensate the distortion of the curves induced by another parameter indicate that the found set of parameters is certainly not unique and will have to be confirmed by some other experiments (optical and mechanical experiments).

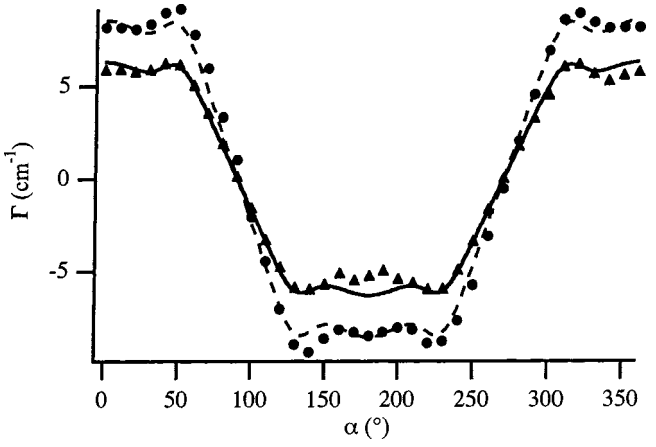

FIG. 11. Comparison between simulations with optimized parameters (full and dashed lines) and experimental results for the B69 (triangles) and B76 (dots) crystals with extraordinary polarization.

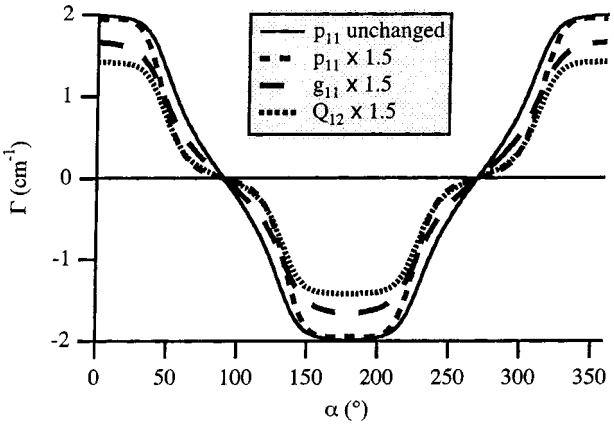

FIG. 12. Influence of the most significant parameters.

D. Additional experiments in 45° cut sample

The orientation of the crystal we use does not bring us any information on r_{42} (or g_{44}^S). It is known that in order to be influenced by r_{42}, we should have $\beta \neq 0°$ and extraordinary polarized beams. We thus performed a rotation measurement in a 45°-cut sample. The crystal studied is a rhodium and sodium doped BCT with 2000 ppm of rhodium and 2000 ppm of sodium labeled B92. The crystal was roof cut to prevent oscillation in the crystal[20] and its thickness is $\ell = 4.1$ mm.

The expected measurement was, nevertheless, not possible with this crystal. Indeed, the photorefractive gain was too high in this configuration to allow a reliable measurement of the gain. A typical energy transfer experiment is shown in Fig. 13. After a normal increase of the intensity of the signal beam, we reach a maximum after which the signal decreases. This decrease is due to the beam fanning that

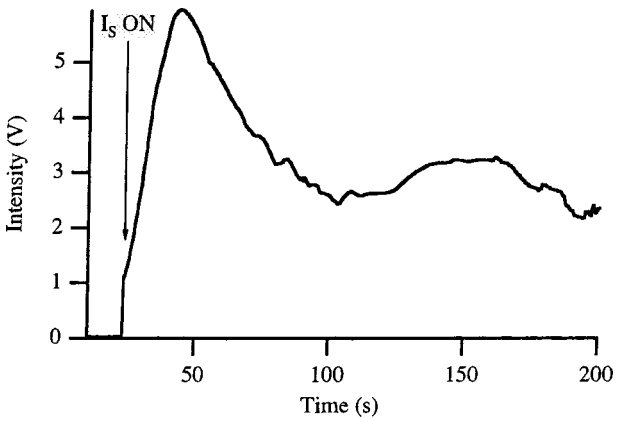

FIG. 13. Energy transfer with extraordinary polarized beams in the B92 crystal.

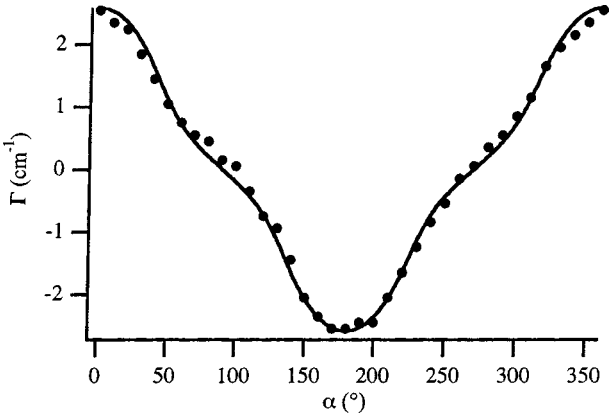

FIG. 14. Comparison between simulations (full line) and experimental results (dots) for gain as a function of the rotation angle α for the B92 45°-cut crystal with ordinary polarizations.

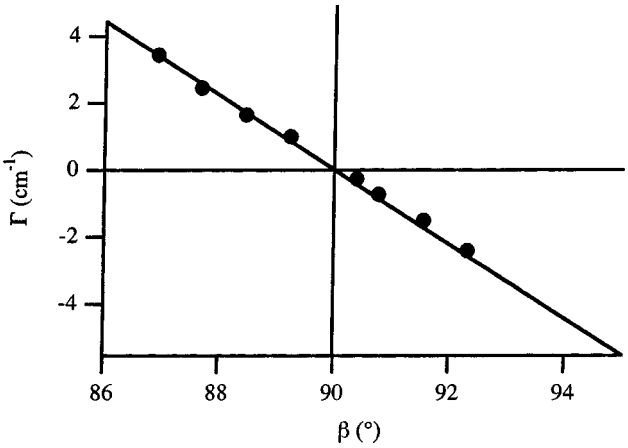

FIG. 15. Gain as a function of β around $\pi/2$ (comparison with simulations).

appears due to the high gain of the crystal, leading to a decrease of the intensity of the pump beam and perturbation of the energy transfer measurement. This phenomenon, which is good news concerning the photorefractive performances of BCT, prevents any measurement with extraordinary polarization in the crystal. The solution for further experiments would be to use a thinner crystal to reduce the gain, with the problem of the technical realization of the crystal (problem for cutting and poling such a thin 45°-cut crystal).

We were, nevertheless, able to perform a measurement in this sample with ordinary polarized beams for which the gain is smaller (Fig. 14). A comparison of the experimental curves with the theoretical curves calculated with the newly determined set of parameters shows a good accordance without changing any parameter and using a reduction factor of 0.52.

This measurement thus confirms our set of parameters but does not give us the expected information about r_{42}. Therefore, we develop another method to evaluate this parameter.

E. Evaluation of r_{42}

To determine r_{42}, we have to perform measurements with $\beta \neq 0$ and extraordinary polarized beams [Eq. (16)]. Using a 0°-cut crystal, one solution would be to go from a configuration with $\beta=0$ with two beams symmetrically incident on the crystal and to rotate the crystal around the vertical axes to have a dissymmetrical incidence of the beam. Unfortunately, due to the rather low value of r_{42} and the relatively large value of the refractive index preventing attaining large values of β, this measurement leads to low variation of the gain and thus to a bad precision in the determination of r_{42}. We thus choose to perform a measurement around $\beta=\pi/2$ with extraordinary polarization. In that case, if β equals exactly $\pi/2$ the photorefractive gain is zero, but as soon as the angle departs from $\pi/2$, the absolute value of the gain increases and we measure a linear variation of the gain with the angle with a slope roughly proportional to r_{42}^T.[4] The measurement is performed in the B69 sample with $k_r = 4\ \mu\mathrm{m}^{-1}$ and is presented on Fig. 15.

If we take into account the factor of reduction of the gain of 0.5 that was measured in this crystal (cf. Sec. IV C), we perfectly adjust the theoretical expression with the experimental data by changing the g_{44}^S value to $g_{44}^S = 0.135\ \mathrm{m}^4\ \mathrm{C}^{-2}$. As in the previous measurements, some parameters have little influence on the theoretical curve; this is the case here for p_{66}^p and s_{66}^p.

F. Electro-optic and piezoelectric coefficients of BCT

To sum up the results of the different adjustments, we have used the orientation dependence of the photorefractive gain to pinpoint the mechanical and optical characteristics of BCT. This adjustment is performed on the cubic phase parameters of BCT (Table I, column 2). They are then used to calculate the tetragonal phase coefficients (Table II). If we compare these values with some available in the literature, especially for the electro-optic coefficient, we observe a good agreement for r_{13}^T and r_{33}^T which measured values were 36 $\mathrm{pm\,V^{-1}}$ and 140 $\mathrm{pm\,V^{-1}}$, respectively.[21] For the third electro-optic coefficient r_{42}^T the difference is more important with the value of 190 $\mathrm{pm\,V^{-1}}$ given in the literature.[22]

To this list of parameters we have to add two other coefficients that are more specific to the photorefractive effect. In Sec. II, we presented measurements of the gain as a function of the grating wave vector in a configuration where $\beta=0$, that allowed us to determine two electro-optic coefficients that were identified then to r_{13} and r_{33}. Following the rest of the study indicating that the indirect electro-optic effect has to be taken into account, we now know that the determined coefficients were in reality $r_{22}^{\mathrm{eff}}(0,0)$ and $r_{33}^{\mathrm{eff}}(0,0)$ respectively. Using the values of the coefficients given in Table II, we calculate their theoretical values that are $r_{22}^{\mathrm{eff}}(0,0) = 34\ \mathrm{pm\,V^{-1}}$ and $r_{33}^{\mathrm{eff}}(0,0) = 107\ \mathrm{pm\,V^{-1}}$. These values are in good agreement with the experimental values given in Sec. II C, $r_{22}^{\mathrm{eff}}(0,0) = 44\ \mathrm{pm\,V^{-1}}$ and $r_{33}^{\mathrm{eff}}(0,0) = 110\ \mathrm{pm\,V^{-1}}$, if we correct these values from the reduction factor of 50% existing in the B69 crystal used in the experiment.

TABLE II. Final tetragonal phase parameters deduced from the cubic phase parameters of Table I.

Clamped dielectric constants		Spontaneous polarization ($C\,m^{-2}$)	
ϵ_{11}^S	824	P_S	0.30
ϵ_{33}^S	140	Elasto-optic coefficients at constant field	
Elastic stiffness at constant field ($\times 10^{10}\,N\,m^{-2}$)		p_{11}^E	0.34
		p_{12}^E	0.08
c_{11}^E	22	p_{13}^E	0.25
c_{33}^E	18.7	p_{31}^E	0.02
c_{12}^E	13.7	p_{33}^E	0.80
c_{13}^E	14.6	p_{44}^E	0.89
c_{44}^E	8.3	p_{66}^E	−0.30
c_{66}^E	11.2	Piezoelectric coefficients ($C\,m^{-2}$)	
Piezoelectric coefficients ($pm\,V^{-1}$)			
d_{31}	−51	e_{31}	−1.42
d_{33}	114	e_{33}	6.52
d_{24}	178	e_{24}	14.7
Unclamped electro-optic coefficients ($pm\,V^{-1}$)		Clamped electro-optic coefficients ($pm\,V^{-1}$)	
r_{13}^T	33	r_{13}^S	26
r_{33}^T	170	r_{33}^S	81
r_{42}^T	453	r_{42}^S	295

G. Optimum configuration for photorefractive gain in BCT

Thanks to this set of parameters, we are now able to calculate the shape of the gain as a function of the angles β and θ [Fig. 16(a)]. We see that the gain is maximum for an angle β of 45° and an angle θ of 9°. For this configuration, the gain should be as high as 78 cm^{-1} at 514 nm. Considering the factor of reduction of the gain of 50%, it means that we can experimentally reach a gain of 39 cm^{-1}.

We have tested the influence, on the position of this maximum, of the values of p_{66}^p and s_{66}^p which are the less known coefficients. If we multiply p_{66}^p by 2, the maximum of gain is then obtained for $\theta=9°$ and $\beta=44°$. If we multiply s_{66}^p by 2, the maximum of gain is obtained for $\theta=9°$ and $\beta=44°$. Therefore, the influence of these parameters on the configuration which maximizes the gain is insignificant.

As expected, the Kerr coefficients have a large influence on the position of the maximum of gain. Indeed, with the initial parameters list (Table I, first column), we obtained a maximum gain for $\theta=12°$ and $\beta=0°$ [Fig. 16(b)]. The experiments presented in this article are thus essential because they have enabled us to determine that the maximum gain can be obtained when the angle between the c axis of the crystal and the grating wave vector is 45°, as was the case for $BaTiO_3$. This last point is confirmed by the fact that we have been able to implement a DPCM only in a 45°-cut crystal (and not in a 0°-cut crystal with the same thickness).[23]

V. CONCLUSION

We performed a two-beam coupling characterization of the BCT crystal, as a function of the spacing and orientation of the written grating, for ordinary polarization. We show that the grating spacing dependence can be interpreted without the need for the indirect electro-optic effect, but this can lead to incorrect values of the deduced parameters. To go further, other experiments should be realized. We choose to study the two-beam coupling as a function of the grating orientation that was successfully used in $BaTiO_3$ and $KNbO_3$, to show the influence of the indirect electro-optic effect. This influence of the indirect electro-optic effect was also observed in BCT, together with a still unidentified effect that reduces the gain. This reduction is independent of the orientation but varies from sample to sample.

Using a model we developed, that calculates the BCT parameters in the quadratic phase (Pockels electro-optic, elasto-optic, piezoelectric, elastic stiffness coefficients) as a function of the parameters in the cubic phase (Kerr electro-optic, elasto-optic, electrostriction, elastic stiffness coefficients), these experimental data are adjusted to make an

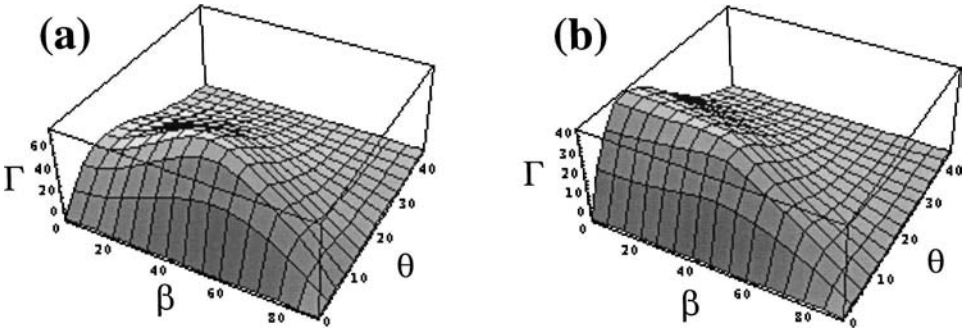

FIG. 16. Three-dimensional plot of the gain as a function of θ and β for the final (a) and the initial (b) set of parameters.

evaluation of these parameters. These results lead to values of $r_{13}^T = 33\,\mathrm{pm\,V^{-1}}$ and $r_{33}^T = 170\,\mathrm{pm\,V^{-1}}$ that are in agreement with previously published values, whereas we reevaluate the value of r_{42}^T to the higher value of $r_{42}^T = 465\,\mathrm{pm\,V^{-1}}$, that confirms the interest of the BCT crystals compared to the $BaTiO_3$.

The values for the different coefficients of the BCT determined here allows us to calculate the optimum orientation for the use of this crystal. We found that the best cut for BCT is a 45° cut as for $BaTiO_3$. This was confirmed by the observation of beam fanning and the implementation of a DPCM in a 45°-cut BCT sample.

ACKNOWLEDGMENTS

L. Mize would like to thank the National Science Foundation International REU Program. Dr. R. Pankrath (University of Osnabrück) is gratefully acknowledged for the growth of the crystals and Dr. D. Rytz (F.E.E. GmbH) for their preparation.

[1] M. Zgonik, K. Nakagawa, and P. Günter, J. Opt. Soc. Am. B **12**, 1416 (1995).
[2] N. V. Kukhtarev, V. B. Markov, S. G. Odulov, M. S. Soskin, and V. L. Vinetskii, Ferroelectrics **22**, 949 (1979); **22**, 961 (1979).
[3] G. Montemezzani, Phys. Rev. A **62**, 053803 (2000).
[4] S. Bernhardt, P. Delaye, H. Veenhuis, D. Rytz, and G. Roosen, Appl. Phys. B: Lasers Opt. **70**, 789 (2000).
[5] Ch. Kuper, R. Pankrath, and H. Hesse, Appl. Phys. A: Mater. Sci. Process. **65**, 301 (1997).
[6] M. B. Klein and G. C. Valley, J. Appl. Phys. **57**, 4901 (1985).
[7] F. P. Strohkendl, J. M. C. Jonathan, and R. W. Hellwarth, Opt. Lett. **11**, 312 (1986).
[8] P. Tayebati and C. Mahgerefteh, J. Opt. Soc. Am. B **8**, 1053 (1991).
[9] J. E. Ford, Y. Fainman, and S. H. Lee, Appl. Opt. **28**, 4808 (1989).
[10] J. F. Nye, *Physical Properties of Crystals* (Oxford University Press, Oxford, 1957).
[11] G. Pauliat, P. Mathey, and G. Roosen, J. Opt. Soc. Am. B **8**, 1942 (1991).
[12] P. Günter and M. Zgonik, Opt. Lett. **16**, 23 (1991).
[13] M. Zgonik, P. Bernasconi, M. Duelli, R. Schlesser, P. Günter, M. H. Garrett, D. Rytz, Y. Zhu, and X. Wu, Phys. Rev. B **50**, 5941 (1994).
[14] A. F. Devonshire, Philos. Mag. **42**, 1065 (1951).
[15] M. DiDomenico, Jr. and S. H. Wemple, J. Appl. Phys. **40**, 735 (1969).
[16] M. Simon, F. Mersch, C. Kuper, S. Mendricks, S. Wevering, J. Imbrock, and E. Krätzig, Phys. Status Solidi A **159**, 559 (1997).
[17] P. Bernasconi, M. Zgonik, and P. Günter, J. Appl. Phys. **78**, 2651 (1995).
[18] F. Jona and G. Shirane, *Ferroelectric Crystals* (Pergamon, New York, 1962).
[19] E. J. Huibregtse, W. H. Bessey, and M. E. Drougard, J. Appl. Phys. **30**, 899 (1959).
[20] N. Huot, J. M. C. Jonathan, D. Rytz, and G. Roosen, Opt. Commun. **140**, 296 (1997).
[21] C. Kuper, K. Buse, U. van Stevendaal, M. Weber, T. Leidlo, H. Hesse, and E. Krätzig, Ferroelectrics **208,209**, 213 (1998).
[22] J. Neumann, N. Rowe, H. Veenhuis, R. Pankrath, and E. Krätzig, Phys. Status Solidi B **215**, R9 (1999).
[23] S. Bernhardt, L. Mize, P. Delaye, R. Pankrath, O. F. Schirmer, and G. Roosen, OSA Trends Opt. Photonics Ser. **62**, 504 (2001).